DESIGN OPTIMISATION OF A BOUNDARY LAYER INGESTION PROPULSOR FOR A MULTI-FUEL HYDROGEN AIRCRAFT

Andrea Battiston[1], Andrea Magrini[1,2], Rita Ponza[1], Ernesto Benini[1,2], Barlas Türkyilmaz[3], Arne Seitz[3] & Alexander Heidebrecht[4]

[1]Hit09 S.r.l.
[2]Università Degli Studi di Padova
[3]Bauhaus Luftfahrt
[4]TU Delft

Abstract

New aircraft concepts leveraging different low emission technologies are expected to drive the transition towards carbon neutrality of the aviation by the mid of the century. This paper presents the preliminary design of a Boundary Layer Ingestion propulsor for a multi-fuel passenger aircraft concept, conceived within the HOPE project. By combining hydrogen-fed Fuel-Cell Auxiliary Propulsion and Power Unit driving a tail cone thruster and multi-fuel combustor enabling sustainable aviation fuel, the new concept aims at minimizing the overall pollutant emissions over the entire mission. The paper describes the general aircraft architecture and technology, showing the results of an initial numerical design study of the tail propulsor.

Keywords: Boundary Layer Ingestion (BLI), multi-fuel aircraft, hydrogen, aircraft design, HOPE Clean Aviation

1. Introduction

International institutions are devoting considerable efforts to push the transition of the aviation sector towards the mid of the century goal of net zero carbon emissions. Among the pillars of this path, new airframe and engine technologies play a significant role. The combination of evolutionary and revolutionary designs is expected to contribute to about 30% reduction of emissions for single-aisle aircraft, relative to the current benchmark [1]. Among these, mixing different energy sources to be adopted in different mission phases, in order to guarantee the necessary energy density while minimising the emissions, can represent a viable option [2]. In addition, futuristic architectures with boundary layer ingestion (BLI) offer theoretical gains in fuel burn around 10-15% [5]. This paper presents a design optimization framework of a Boundary Layer Ingestion propulsor for a multi-fuel passenger aircraft. The narrow-body tube and wing configuration features an integrated propulsion system comprising two multi-fuel ultra-high bypass ratio (UHBR) turbofan engines in under-wing installation and a hydrogen fuel cell based auxiliary propulsion and power unit (FC-APPU) driving an aft-fuselage BLI propulsor [8].

With such a complex architecture and a deep integration and inter-operation of the components, aircraft sizing, engine design, and BLI propulsor installation become major challenges. In order to efficiently combine and operate all systems, numerical optimisation algorithms are essential to find constrained minima of highly multivariate functions determining the overall aircraft performance. In this paper, we present a numerical framework that adds to the preliminary aircraft design the higher fidelity level of CFD simulations aimed at optimising the BLI propulsor installation in the aft fuselage, considering aerodynamic, propulsive, safety, and operational constraints. After introducing the numerical framework, the results of the aft fuselage propulsor optimisation are discussed, illustrating aerodynamic and propulsive characteristics of the final optimised geometry.

2. HOPE Technology Aircraft

By combining multi-fuel capable UHBR turbofan engines with hydrogen fuel cell powered fuselage BLI propulsion, the HOPE technology aircraft concept aims at a best and balanced design for minimum noise and emissions at all stages of aircraft movement. The hydrogen FC-APPU powered BLI propulsor is targeted to enable zero-emission taxi as well as ultra-efficient cruise performance. The UHBR turbofans are intended to allow for the capability of flexibly burning mixtures of kerosene or Sustainable Aviation Fuels (SAF) and hydrogen, thereby lifting hydrogen's advantages with regard to low emissions and enhanced efficiency while minimising its intrinsic penalties due to the greatly extended demand for storage volume. The overall aircraft concept is illustrated in Fig. 1.

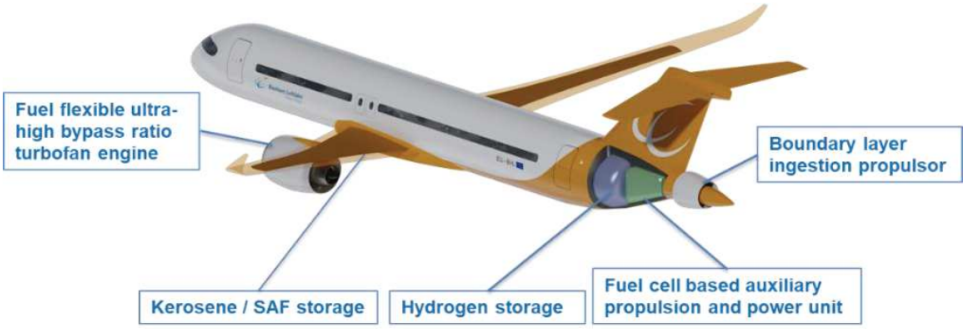

Figure 1 – Multi-fuel aircraft architecture studied in the European funded project HOPE. Credit: BHL for providing the aircraft visualization.

The vehicle is based on a tube-and-wing aircraft layout with a T-tail arrangement. The multi-fuel UHBR turbofan engines are conventionally under-wing podded. The BLI propulsive device is located at the aft-fuselage, behind the trailing edge of the vertical fin. The FC-APPU and the liquid hydrogen (LH_2) storage tank are placed inside the fuselage between the BLI propulsor and rear pressure bulkhead. Key aircraft design characteristics as well as important requirements for the BLI propulsor design are discussed and derived in the following.

2.1 Key Aircraft Design Characteristics

The HOPE technology study focuses on the classic short-medium-range (SMR) market segment, i.e. an A320neo-class aircraft with a baseline scenario of advanced technologies tailored to reflect a potential entry-into-service (EIS) in 2035. The aircraft-level technology evaluation is performed following a rigorous, methodical approach based on a consistent set of meaningful top-level aircraft requirements (TLARs). A selection of key TLARs relevant for the BLI fan design is provided in Table 1.

Table 1 – Selected Top-Level Aircraft Requirements (cf. [4])

Parameter	Requirement
Entry into service	2035
Design range	3000 NM
Design payload	18000 kg
Cruise Mach	$\geq$ 0.76
Max. operating Mach	0.82
Initial cruise altitude	$\geq$ FL330
Max. operating altitude	FL410
Airport compatibility	ICAO Code C
LTO NO_x emissions	-70% cf. CAEP/8
LTO noise	-3 EPNdB per operation cf. A320neo
Climate impact	-30% cumulative cf. A320neo

The above listed TLARs form the basis for the design and performance assessments of all HOPE aircraft. While most of the performance related requirements, such as the payload range capacity

and design cruise conditions are in line with current SMR aircraft, the advanced environmental requirements including landing- and take-off (LTO) NO_x and certification noise have additional impact on the specification of the propulsion system, especially the design and operational patterns of the BLI propulsive device, e.g. during taxi and LTO cycle.
The aircraft-level studies to assess the potential of the HOPE technology is conducted using the Bauhaus Luftfahrt Aircraft Design Environment (BLADE) [3], which was built with modularity, transparency and automation in mind to facilitate consistent aircraft designs. The study baseline is formed by a year-2035 projection of the BHL A320neo-class aircraft forming the baseline aircraft, described in further detail by Türkyilmaz et al. [4]. Building upon this baseline design, the HOPE propulsion system technologies will be introduced in a stepwise manner, as the project progresses. Dedicated steps will include an intermediate aircraft design featuring the multi-fuel turbofan engines alongside an H_2 fuel cell auxiliary power unit (FC-APU) serving aircraft subsystems power demands during aircraft operation, as well as a final design with an even more powerful fuel cell system (FC-APPU) sized to also drive the BLI propulsor at the rear fuselage.

2.2 Basic Requirements for BLI Fan Design

Starting from the set of TLARs and and an initial sizing of the baseline aircraft, a number of basic constraints and target performance figures for the design space exploration of the BLI propulsor were derived at the beginning of the HOPE project. These include estimated fan power settings for selected relevant operating conditions as well boundary conditions to be considered for the geometric sizing and integration of the BLI propulsive device.

2.2.1 Main Geometric Bounds

One constraint on the rear propulsor design emerges from the ground clearance requirement during take-off. The ducted propulsor may not limit the take-off rotation angle of the aircraft, which means that it must be geometrically positioned above the line originating at the extended landing gear and tangent to the rear fuselage tailcone. A typically required angle during take-off rotation (i.e. with extended, uncompressed main landing gear) is $\geq 12°$. This natural constraint is further pronounced in the HOPE aircraft configuration because of expected fuselage length increments due to the integration of the LH_2 storage together with a given single-aisle passenger cabin configuration.
It should also be noted that regulations [9] require that the airplane be able to take off after a tailstrike, with fully deflected elevators. This causes the tail to scrape along the runway even after the landing gear has lifted off, which means that the entire convex hull of the tailcone geometry from the point of impact of the initial tailstrike to the downstream end may come into contact with the ground. While the forces acting on the tail during this maneuver are modest compared to the initial impact, it is possible that the lower part of the nacelle will require some reinforcement for this scenario. It may also be beneficial to add replaceable "pads" with suitable ablative properties in critical locations, in order to avoid rivets or other smaller pieces being sheared off and ingested into the rear engine. An alternative could be an automatically-deployed device which could prevent direct contact between the skin panels and the ground after a tailstrike.
Another key geometric constraint for the sizing of the aft-fuselage BLI propulsor is the minimal hub diameter at the rotor plane. Assuming a ducted propulsive device, in the first instance, the mechanical complexity of the nacelle should be kept to a minimum. As a result, the transfer of the aerodynamic, inertial and gyroscopic loads across the fuselage BLI fan rotor plane will be best realized by the structural load path routed through the fan rotor hub. This allows for the least number of structural items in the fuselage inflow streamtube, and, it enables a complete structural decoupling from loads introduced by the empennage. In HOPE, an aero-structural integration and mechanical design arrangement inside the fuselage fan hub is assumed that is similar to the conceptually designed in the CENTRELINE project. A representation of the geometric arrangement of this fuselage fan rotor system including electric drive motor, bearings, and internal support structure is presented by Seitz et al. [10]. The determination of a minimum allowable hub diameter of the fuselage fan flow path requires the consideration of minimum required rotor disk bore radii as well as the inner and outer bearing radii as key design constraints. In order to obtain a first estimate for the HOPE design case, conceptual design solutions from CENTRELINE (cf. [10]) were scaled based on the expected ideal

fuselage fan shaft power levels in cruise. In result, the hub-to-tip ratio of the fuselage fan rotor should not fall below approximately 0.4.

2.2.2 Target Performance Properties

A key parameter for the BLI fan sizing and performance prediction are the target power levels to be absorbed by the fan rotor at key operating conditions. A convenient figure of metric to initially determine meaningful fuselage fan power at its aerodynamic design point, i.e. typical cruise conditions, is the so-called Power Saving Coefficient (PSC) that was initially proposed by L.H. Smith [11]. The PSC relates the power supply required to operate an aircraft with and without BLI propulsion. Seitz et al. [12] provide straight-forward analytical formulation in order to assess the PSC for aircraft configurations featuring a single aft-fuselage BLI fan. Accordingly, the PSC can be calculated based on small number of propulsion system efficiency figures that can be initially estimated based on experience, and, basic knowledge about the aerodynamic characteristics of the baseline aircraft without BLI propulsion. Synopses of these properties and correspondingly assumed initial values for the HOPE technology application case are presented in Tables 2 and 3.

Table 2 – Typical cruise characteristics of baseline aircraft (without BLI)

Property	Value
Flight Mach number	0.78
Flight altitude	FL350
Instantaneous gross weight	61 t
Lift/drag	18
Fuselage drag / total drag	0.25

Table 3 – Initially estimated propulsion system efficiency figures at typical cruise conditions

Property	Value
Effective propulsive device efficiency[a]	0.73
Effective core efficiency[a]	0.53
APPU fuel cell system efficiency	0.50
Fuselage BLI fan electrive drive train efficiency	0.97
Fuselage BLI fan polytropic efficiency[b]	0.93

[a] underwing podded engines, [b] -1% relative to non-BLI fans

Using the parameter values tabulated above and applying the non-dimensionalised heuristic formula for the bare propulsive fuselage efficiency factor presented by Seitz et al. [10]), a preliminary evaluation of maximum PSC and correspondingly optimum shaft power inputs to the ducted BLI fan at typical cruise can be performed for the HOPE technology case. Therefore, the fuselage fan ideal shaft power input (i.e. BLI disc power) can be varied within meaningful ranges, while retaining the invariant properties of the underlying baseline aircraft without BLI propulsion. In case design properties of the baseline aircraft change, this can be emulated through adequate changes in the property values listed in Table 2.

The results of an initial parametric study for optimum power savings with a ducted BLI propulsive device in HOPE is shown in Fig. 2. In the presented study, the overall fuselage length of the baseline aircraft is treated as an array parameter, in order to identify the sensitivity of maximum power savings and correspondingly optimum BLI fan power input in cruise against the implications of hydrogen tank size.

The study in Fig. 2 indicates optimum BLI fan disc powers around the 3 MW range, slightly increasing with extending fuselage length. Maximum PSC values range between 6% and 7% for the given study settings.

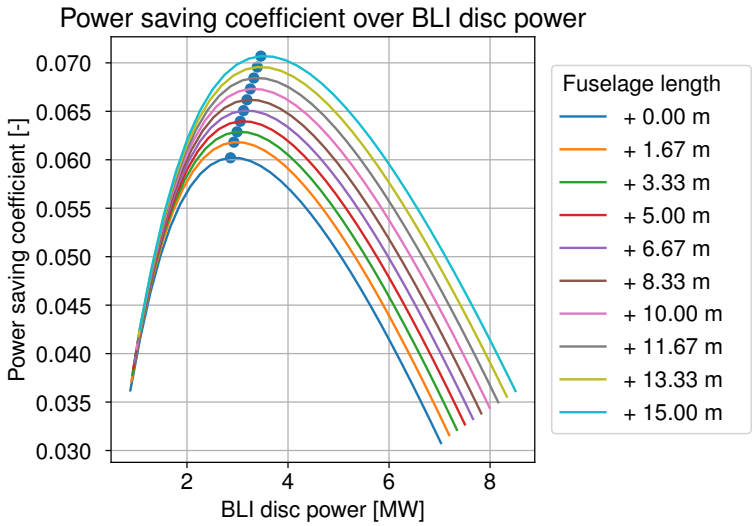

Figure 2 – BLI fan power study for optimum power savings in typial cruise (A): Sensitivity to baseline fuselage length

As a second initially estimated input setting with crucial impact on both attainable PSC and correspondingly optimum BLI fan disc power in cruise is the efficiency of the APPU fuel cell system, i.e. the fuel cell stack with the entirety of its balance of plant components included. A parametric study similar to the previous one, however with deltas in APPU fuel cell system efficiency now used as the array parameter, is presented in Fig. 3.

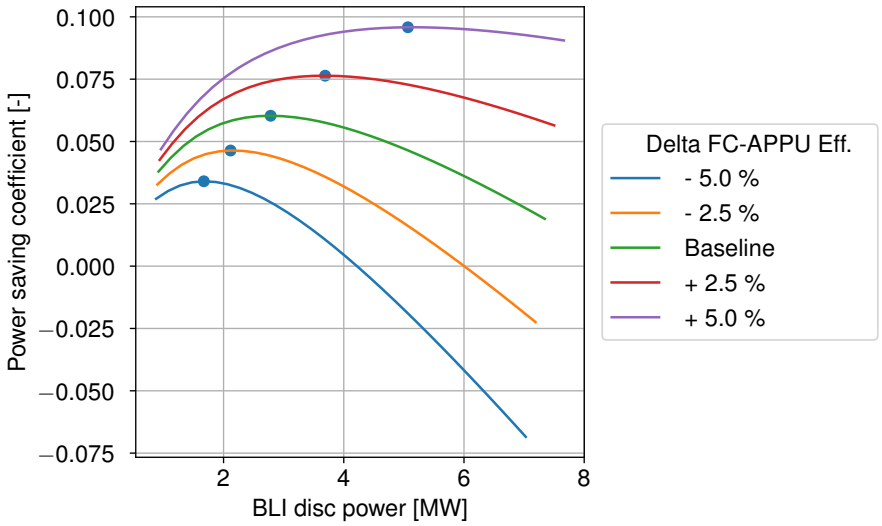

Figure 3 – BLI fan power study for optimum power savings in typial cruise (B): Sensitivity to change in APPU fuel cell system efficiency

For the study shown in Fig. 3, APPU fuel cell efficiency was effectively varied between more conservative 45% and more aggressive 55% values for typical polymer electrolyte fuel cells. The significant influence of this variation on both, achievable PSC and correspondingly optimum BLI fan disc powers, the latter of which range between slightly below 2 MW for the lowest APPU efficiency value and approximately 5 MW at its highest. With the assumed APPU system efficiency goal of 50%, in cruise, 3 MW is confirmed as a adequate initial target level of ideal shaft power input for the BLI fuselage fan design, in HOPE. Taking into account best and balanced sizing and operating strategies for a fuel cell APPU (cf. Kolb et al. [13]), 3 MW represents a meaningful limit for BLI fan power input, also for

maximum climb and maximum take-off ratings.

3. BLI Propulsor Design and Optimization

The BLI propulsor design was carried out by using the following sequential approach:

1. Definition of consistent metrics for the performance evaluation;
2. Definition of a three-dimensional parametric geometry based on a coherent set of design variables;
3. Design space exploration, aimed at understanding the influence of the design variables on the propulsor performance;
4. Optimization of the BLI propulsor.

3.1 Performance Evaluation

The determination of a consistent performance metric is relevant and cannot follow the conventional momentum conservation approach used for classic podded engines. Although a clear distinction between thrust and drag forces cannot be determined, it is also apparent that a force balance can still be valid when considering the overall architecture. The proposed performance accounting has been defined considering the overall airframe force [6]. Denoting with F_{Sx} the wall forces acting on the surfaces, and with F_{Gx} the gauge forces at the fan sections, their components on the streamwise direction $\hat{x}$ can be evaluated as:

$$F_{Sx} = \int_{S_w} \left[(p - p_\infty)\,\hat{n} + \vec{\tau}_w \right] \cdot \hat{x} dS \tag{1}$$

$$F_{Gx} = \int_{A} \left[(p - p_\infty)\,\hat{n} + \rho \vec{V} \left(\vec{V} \cdot \hat{n} \right) \right] \cdot \hat{x} dA \tag{2}$$

A Net Assembly Force NAF is therefore defined by taking the sum of all the forces acting on the airframe. Note that a half-model aircraft comprising the entire fuselage with the aft propulsor, the wing, and the vertical tail plane is used in the study, as shown in Fig.7. Being A the fan intake section and E the fan exhaust section:

$$NAF = F_{Sx,tot} + F_{Gx,A} + F_{Gx,E} \tag{3}$$

From this parameter, a surrogate of the net propulsive thrust is introduced, by subtracting to the Net Assembly Force a reference drag:

$$\Delta NAF = NAF - D_{ref} \tag{4}$$

This force takes into account the installation effects of the BLI nacelle and the variations in the fuselage shape with reference to a non-BLI configuration. From this force, a surrogate of the propulsive efficiency has been defined, as the ratio between the apparent propulsive power related to ΔNAF and the fan mechanical flow power:

$$\xi_p = \frac{-\Delta NAF\, V_\infty}{W_{fan}} \tag{5}$$

3.2 Geometric Parametrization

The geometry was parameterized considering a large set of design variables and different typologies of curves, with C^1 or C^2 continuity enforced at their connection. Figure 4 depicts the parametric geometry.

In particular, the nacelle lip was composed of two Bézier curves, each one defined by four control points. Both curves are constrained at the leading edge with a variable curvature radius, which guides the second control point of each curve. The introduction of a common curvature radius between the two curves consented the definition of the nacelle lip based on three design variables: the leading edge curvature radius and the horizontal displacements of the points P_2 and Q_2, as sketched in

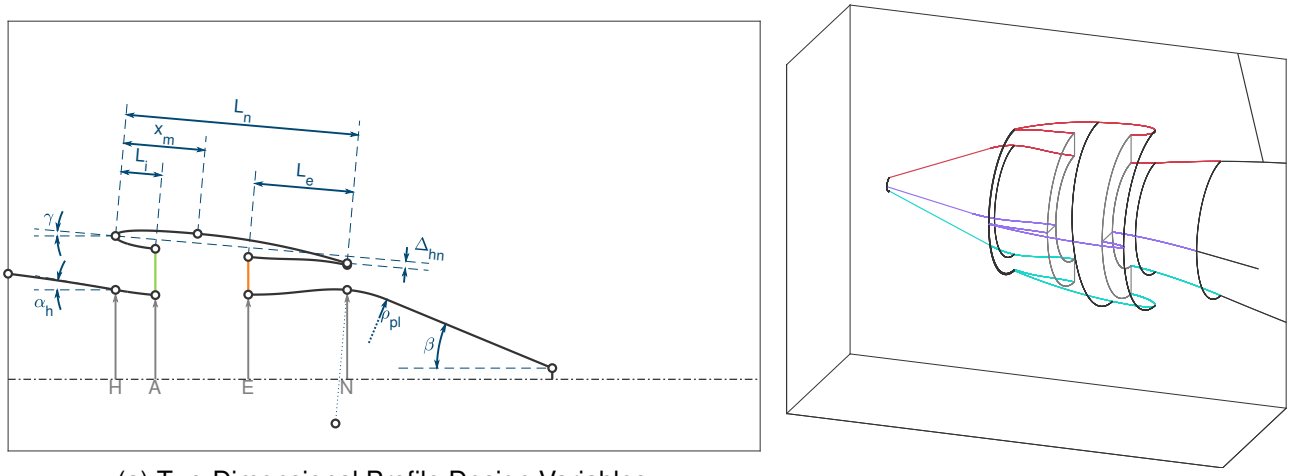

(a) Two-Dimensional Profile Design Variables

(b) Three-Dimensional View

Figure 4 – Parametric Geometry

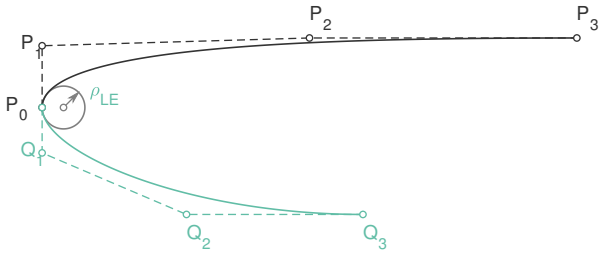

Figure 5 – Leading Edge Parametrization

Figure 5.

Denoting a Bézier curve as $\vec{B}(u)$, the curvature can be evaluated as:

$$\kappa(u) = \frac{1}{\rho(u)} = \frac{||\ddot{\vec{B}}(u) \wedge \dot{\vec{B}}(u)||}{||\dot{\vec{B}}(u)||^3} \tag{6}$$

In the assumption that, at the leading edge ($u = 0$), the Bézier polygon features a vertical segment (hence $x_0 = x_1$ for both P_1, Q_1), solving the above equation for the vertical position y_1 of P_1 (or Q_1) leads to:

$$y_1 = y_0 \pm \sqrt{\frac{2}{3}\rho_{LE}(x_2 - x_1)} \tag{7}$$

The downstream portion of the outer cowl was defined by a parabolic arc, as well as the intake section hub curves. The exhaust section was parameterized using 5^{th} degree polynomial curves, based on different conditions: the hub curve connected with curvature continuity with the tail plug, which was designed using a circular arc and a straight line, whilst the shroud curve featured a non-zero inclination at the trailing edge.

The two-dimensional parametrization defines the sideline propulsor profile. From such a profile, variations in terms of highlight height and axial position of the maximum cowl radius point were produced for two azimuthal planes at $0°$ (crown) and $180°$ (keel). The three profiles were then connected using circumferential interpolation laws. The axial position of the maximum cowl radius point was interpolated using a 6^{th} degree polynomial curve. The curve boundary conditions were the passage through the points at azimuth $0°, 90° 180°$ and zero first derivative and curvature at the azimuth planes $0°, 180°$, for a total of seven conditions, thus leading to a 6^{th} degree polynomial.

The highlight section was parameterized using two Bézier curves, which defined two portions of the section (from $0°$ to $90°$ and from $90°$ to $180°$). For both sections, the constrained points corresponded to the curve ends, in which the azimuth values and the highlight radii were known. The central control points were set to ensure C^2 continuity.
The geometric constraints described in section 2.2.1were considered in the parametric model: the minimum hub diameter was set as a constant value for each individual. The tail strike angle was granted by considering an opportune range of fan diameters, defined by the hub to tip ratio.

A further design variable was the fan total pressure ratio FPR. In this phase, the fan was modelled as a boundary condition, by targeting the fan pressure ratio and the polytropic efficiency. An automatic updating approach ensured that the fan discharge plane in the CFD model has a total pressure equal to FPR times the AIP total pressure, and a total temperature derived from the assumed constant polytropic efficiency. The mass flow continuity across the fan inlet and fan discharge planes was enforced by changing the AIP static pressure to match the mass flux ejected in the nozzle.

3.3 Mesh Topology and Sensitivity Analysis

The mesh used for the CFD evaluations can be seen in Figure 7. The surface grids were structured or quad-dominant. The volume grid was composed of unstructured blocks filling the external region and structured blocks around the propulsor and the wake. A mesh convergence analysis was carried out to determine the final mesh to be used for the parametric analyses. Figure 6 summarizes the sensitivity study: the mass flow rate and the performance parameters were monitored, and the resulting mesh comprises of ~ 51M elements.

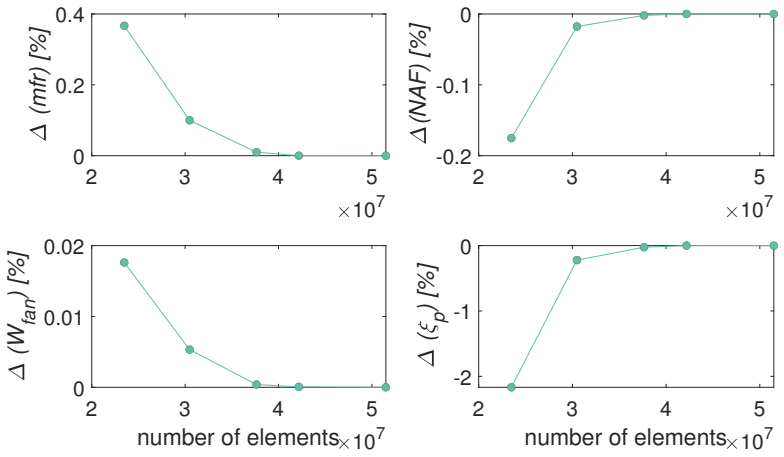

Figure 6 – Parametric Mesh: Sensitivity Analysis

In the CFD analyses, the propulsor was modeled through boundary conditions at the fan inlet (A) and exhaust (E) sections, with a one-dimensional modelling of the fan stage achieved by imposing a the fan inlet boundary (set as a pressure outlet) the mass flow rate discharged through the exhaust (set as a pressure inlet), where the stagnation pressure was π_c times the average total pressure at plane A, and the stagnation temperature derived from the assumed fixed fan polytropic efficiency, according to the approach already used in [6]. Averaged parameters over the inlet and outlet boundaries were computed at each iterations and updated until convergence. The assumed efficiency level from the fan was conservatively taken to be 0.89 in the first instance, to account for the effect of ingested wing and vertical tail plane wakes, even if higher values can be targeted with detailed fan design.

3.4 Design Space Exploration

The relevance of the large number of design variables on the performance metrics was assessed in an initial design space exploration aimed to reduce the dimensionality of the design space and

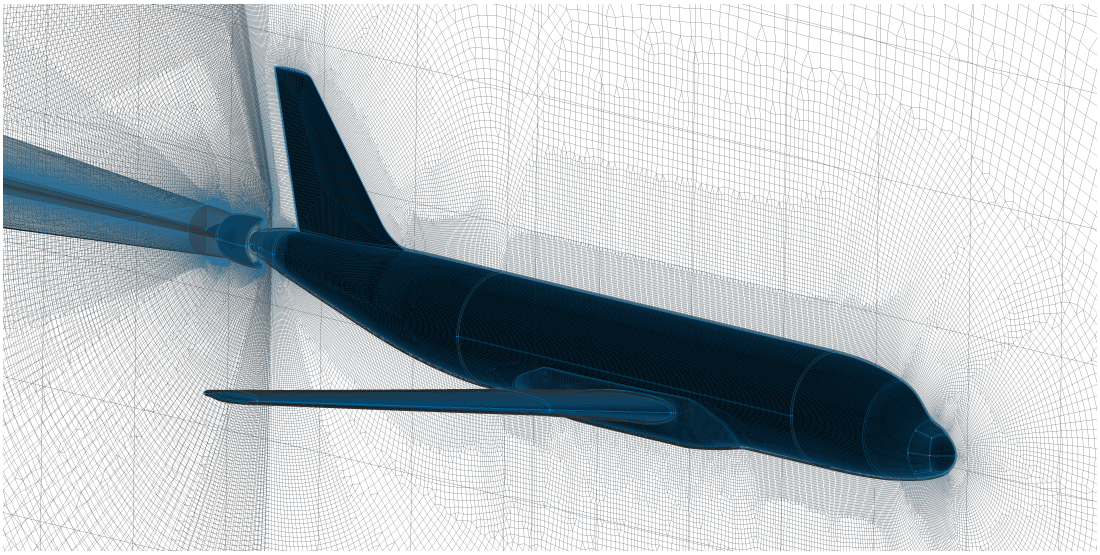

Figure 7 – Parametric Mesh: fixed Airframe and BLI propulsor

Table 4 – Design variables ranges used in the DoE.

Des. Var	Lower bnd.	Upper bnd.	Description
γ	0.000	4.000	Nacelle Cone Angle
L_{nac}/L_{aft}	0.100	0.150	Nacelle Length / Aft-Fuse Length
L_{itk}/L_{nac}	0.150	0.200	Intake Length / Nacelle Length
L_{exh}/L_{nac}	0.400	0.500	Exhaust Length / Nacelle Length
$\Delta x_{m,u}$	0.000	0.025	Max. Cowl Radius: crown profile displacement
$\Delta x_{m,l}$	-0.025	0.000	Max. Cowl Radius: keel profile displacement
$\rho_{LE}/(0.5t_{max})$	0.075	0.200	Normalized Leading Edge Curvature Radius
$\Delta s_{H,u}$	-0.075	0.000	Highlight shroud radius: crown profile displacement
$\Delta s_{H,l}$	0.000	0.075	Highlight shroud radius: keel profile displacement
α_H	0.000	5.000	Highlight Inclination Angle
r_A/s_A	0.450	0.550	Fan Hub to Tip Radius
A_N/A_E	0.500	0.700	Nozzle Contraction Ratio
$w_{CP1,H}$	0.450	0.600	Highlight circumferential law: 1st control point weight
$w_{CP2,H}$	0.450	0.600	Highlight circumferential law: 2nd control point weight
FPR	1.300	1.400	Fan total pressure ratio

downselect only the most influential variables. To this purpose, a Design of Experiments (DoE) based on Latin Hypercube Sampling (LHS) was used. The admissible ranges of the variables is summarized in Table 4.

The quasi-random analysis was carried out considering the aerodynamic design condition from TLARs, with $M_\infty = 0.78$ at an altitude $z_\infty = 10668m$ and an Angle of Attack (AoA) $AoA = 1.5°$. A general picture of the influence of the variables on four main propulsive metrics is depicted in the correlogram plot of Fig. 8. The most influential geometric variables resulted to be the fan hub/tip ratio and the nozzle contraction ratio, which can be clearly understood considering that they determine the amount of ingested boundary layer and thus the overall mass flow and momentum on the exhaust. Noticeably, the fan hub/tip ratio had a lower impact on ξ_p, despite affecting the net thrust through the mass flow rate, and thus the fan power. Other influential geometric variables were those controlling the outer cowl azimuthal contour ($\Delta x_{m,u}$,$\Delta x_{m,l}$, and $w_{CP1,H}$), since the large crown to keel change of the flow field caused by the fuselage upsweep was sensitive to the outer cowl shape and highlight area distribution. These variables determine the drag of the nacelle and thus affected also ξ_p. The fan pressure ratio is also clearly important in setting the net thrust level and the overall fan power. The FPR featured a less significant linear correlation with the efficiency ξ_p than the nozzle contraction

ratio. This is justified by the fact that the chosen range lied within a near-optimum region, as found out by previous design explorations and optimizations on similar architectures[6, 7].
The best individual of the DoE analysis featured a surrogate NAF propulsive efficiency $\xi_p = 0.7810$ with a FPR=1.35. To further improve ξ_p based on the outcome of the correlation study and targeting the available fan power, the nozzle contraction ratio was increased from 0.6952 to 0.75, whilst keeping all the other variables fixed. The resulting configuration had $\xi_p = 0.7989$. Its shape and the correspondent Mach Number contour at the symmetry plane are shown in Figure 9. The image shows the short and slim nacelle obtained, with a nonuniform Mach distribution from crown to keel and the unchoked nozzle due to the moderate FPR and low boundary layer total pressure. The propulsor thus obtained will be further refined in order to locally improve the flow field in the highlight region and optimize the nozzle flow expansion to ensure a stable fan operation insensitive to the discharge conditions.

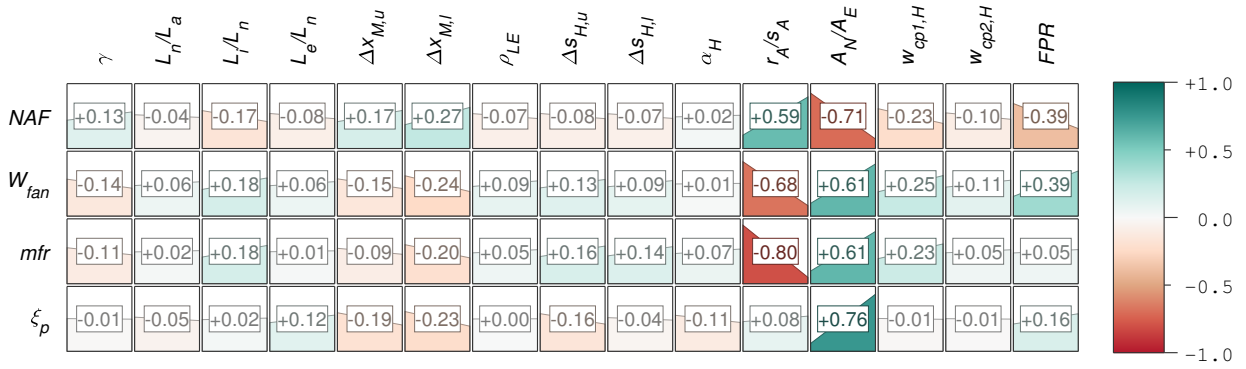

Figure 8 – Design of Experiments: correlation plot.

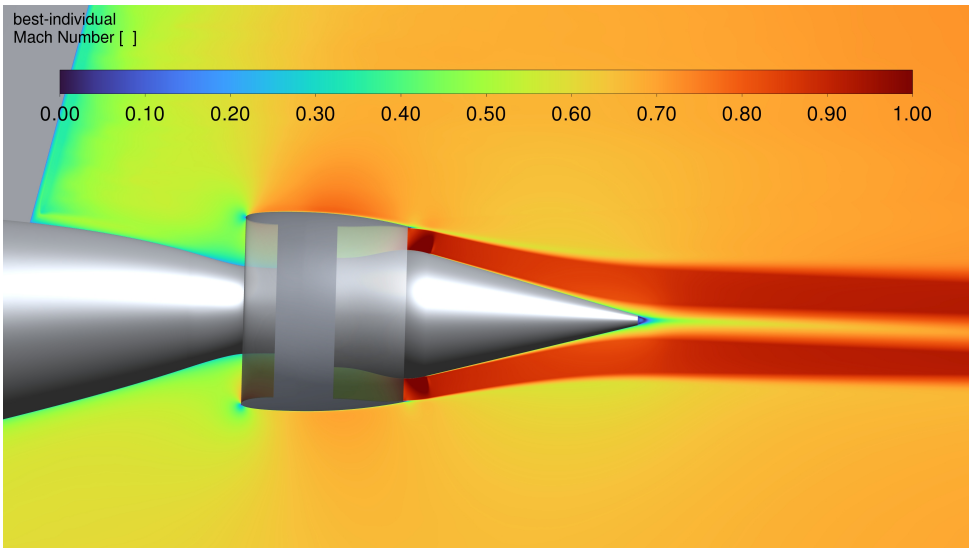

Figure 9 – Mach number contour for best DoE individual.

4. Conclusions

The HOPE project aims to develop a multi-fuel hydrogen-powered aircraft with BLI aft fuselage propulsor. The main aircraft architecture, top level requirements and propulsive system layout have been reported. Due to the complex integration of the different powerplants into the fuselage, the fuselage tail design must adhere to a series of functional, geometric, and safety constraints, to ensure an adequate storage capability and ground clearances, without negatively impacting the airframe and control surfaces sizing. Starting from top level aircraft requirements, an initial configuration has been defined and a numerical investigation of a wing body with vertical tail plane and aft-fuselage BLI engine has

been conducted. The design space exploration highlighted the most influential design variables, that are the highlight area and fan hub/tip ratio, the nozzle contraction ratio, and the nacelle cowl circumferential shape. The resulting low fan pressure ratio BLI propulsor featuring a compact short nacelle will determine the baseline aircraft configuration whose design will be completed, throughout the HOPE project, with the detailed powerplant design for the multi-fuel underwing UHBR turbofans, the hydrogen fed FC-APPU, and the BLI fan stage.

Acknowledgments

This study is financed by the project HOPE. The project has received funding from the European Union's Horizon Programme under GA no. 101096275.

Copyright Statement

References

[1] Clean Aviation. *Strategic Research and Innovation Agenda*. Clean Aviation Joint Undertaking, 2021.

[2] Yin, F., et al., *Performance assessment of a multi-fuel hybrid engine for future aircraft*, Aerospace Science and Technology. 77, 2018.

[3] Michael Lüdemann, *BLADE: A Modular Environment for Traceable and Automated Aircraft Design*, 13th EASN International Conference, Salerno, Italy, Sep. 6 2023.

[4] Barlas Türkyilmaz, Michael Lüdemann, Moritz G. Kolb and Alexandros Lessis, *Definition of a Year-2035 Baseline Aircraft for Short-Medium Range*. Abstract submitted for publication in 14th EASN International Conference, Thessaloniki, Greece.

[5] Nicolas G.M. Moirou, Drewan S. Sanders, Panagiotis Laskaridis, *Advancements and prospects of boundary layer ingestion propulsion concepts*, Progress in Aerospace Sciences, Volume 138, 2023.

[6] Andrea Battiston, Rita Ponza and Ernesto Benini. *Design Exploration for an Axisymmetric Rear BLI Propulsor*, AIAA 2021-3470, AIAA Propulsion and Energy 2021 Forum. August 2021.

[7] Andrea Battiston, Rita Ponza and Ernesto Benini. *Design of a Rear BLI Non-Axisymmetric Propulsor for a Transonic Flight Experiment*, AIAA 2022-3803. AIAA AVIATION 2022 Forum. June 2022.

[8] HOPE Project: https://hope-eu-project.eu/

[9] *Certification Specifications and Acceptable Means of Compliance for Large Aeroplanes (CS-25)*, EASA, Amendment 27, Nov 2021.

[10] Seitz, A., Habermann, A.L., Peter, F., Troeltsch, F., Castillo Pardo, A., Della Corte, B., van Sluis, M., Goraj, Z., Kowalski, M., Zhao, X., Grönstedt, T., Bijewitz, J., and Wortmann, G. *Proof of Concept Study for Fuselage Boundary Layer Ingesting Propulsion*, Aerospace 2021, 8(1). https://doi.org/10.3390/aerospace8010016 .

[11] Smith, L.H. *Wake ingestion propulsion benefit*, J. Propuls. Power 1993, 9, 74–82, doi:10.2514/3.11487.

[12] Seitz, A., Habermann, A.L. , van Sluis, M. *Optimality Considerations for Propulsive Fuselage Power Savings*, Proceedings of the Institution of Mechanical Engineers, Part G: Journal of Aerospace Engineering, 2021;235(1):22-39, first published online, 08 April 2020, https://doi.org/10.1177/0954410020916319.

[13] Kolb, M.G., Seitz, A., Türkyilmaz, B., Ma, Y. and Hornung, M. *"Modelling and Initial Assessment of a Fuel Cell Auxiliary Propulsion and Power Unit*, in 34th Congress of the International Council of the Aeronautical Sciences, Florence, Italy, 09-13 September, 2024.